Numerical Investigation on Performance of Groove-sintered Wicked Heat Pipe

Suroju SaiKumar

M. Tech (Thermal) Student, Department of Mechanical Engineering, Gokaraju Rangaraju Institute of Engineering and Technology, Bachupally, Telangana 500090, India
Email- suroju.sai@gmail.com

B. Ch Nookaraju

Associate Professor, Department of Mechanical Engineering, Gokaraju Rangaraju Institute of Engineering and Technology. Bachupally, Telangana 500090, India

Email- nookarajubch@yahoo.com

Abstract: In this study, a CFD model of groove-sintered wick was developed to investigate the thermal performance of heat pipe and analyze the multi-phase process. A comparison is made between the experimentation and CFD simulation. The design parameter and experiment values were taken from literature and performed CFD analysis. The error was less than 5%. Hence present volume of fluid (VOF) model can effectively reproduce phase change and heat transfer. In this study different porosity is used in the groove-sintered wick to achieve minimum thermal resistance. Thermal behavior is investigated on the porosity values of 35%, 42%, and 50%. The heat input used in the study is varied from 20 to 80W. The results showed that the thermal resistance of wick having a porosity of 35% is the lowest i.e. 0.031K/W. After 60W the thermal resistance is seen increasing in all the cases. Discussions are made on temperature distribution, variation in volume fraction, and velocity vectors.

Keywords: CFD, Groove-sintered wick, Heat pipe.

I. INTRODUCTION

The heat pipe is a heat transfer device that transfers heat from one point to another with the help of the evaporation and condensation principle. Heat pipes are also referred to as superconductors because of their high capability to transfer heat. Heat transfer in heat pipe takes place by conduction and change in the phase of working fluid [1].

With the advancement in technology in the world, electronic devices are becoming miniature and more compact. Reduction in size of chipset makes more generation of the heat and small area restricts the flow of the heat transfer [2]. The smaller the size of the device greater will be the heat generation and the smaller will be the heat transfer coefficient. To address this problem many researchers are working on effective heat dissipation techniques. The heat pipe is the more efficient and low-cost device in removing heat generated by the electronic devices. The capillary driven two-phase system uses the working fluid without mechanical devices and can operate without any maintenance [3].

In this study, the focus is made on the wicked heat pipe, because of their high capillary pressure and permeability. Grove-sintered composite wick is considered for the analysis.

II.LITERATURE REVIEW

Minghan Zhu et al., [4] performed experiments on heat pipe with porous grooved structure. In this study, a composite porous heat pipe with a porous grooved structure is developed and thermal performance is evaluated. The thermal response performance, temperature distributions, effective thermal conductivity, and thermal resistance of CPHP were investigated. Smaller particle size possesses lower permeability and greater capillary pressure. When the size of copper powder particle is decreased, the thermal resistance and power of proposed heat pipe decreased. The maximum heat transport capabilities of samples 120-2, 96-2, and 75-2 are 80 W, 75 W, 60 W, and the corresponding thermal resistances are 0.079 °C/W, 0.066 °C/W, and 0.049 °C/W, respectively.
Lelun Jiang et al., [5] conducted experiments on composite groove-sintered wick flattened heat pipe. In this study, a porous crack composite heat pipe (PCHP) is fabricated by phase change flattening technology and analyzed thermal

performance such as start-up performance, isothermal performance, heat transfer limit, and thermal resistance. It is proved that the performance of the proposed PCHP is much better than the individual grooved and porous heat pipe. The proposed PCHP reaches steady in 10sec whereas for GHP and SHP it took 15 sec to reach a steady state.

Jiayin xu et al., [6] developed the composite wick with a pore size of 48-96μm for the evaporation section and 96-120μm for condensation and transportation. They achieved a heat load of 140W (19.8 W/cm2) without dry out and a maximum heat transfer coefficient of 30,794 W/m2K. The lowest evaporator thermal resistance is 0.046 °C/W at a heat load of 140 W.

Yech-Ju Lin et al., [7] investigated the effects of shape of powder and different parameters on heat dissipation of heat pipes with porous sintered wicks. He found that the capillary speed depends on the pore shape and size. The spherical shape has high permeability and capillary speed and good heat dissipation when compared to the irregular shape of water atomized powder and dendrite shape with electrolytic powder. They showed that the permeability will increase for the powder surface is smooth and proved that surface roughness is more important than pore length and pore shape.

ThanwitNaemsai et al., [8] developed a numerical model for sintered grooved heat pipe and performed FEA analysis and predicted thermal resistance under non-uniform conditions in the thermal module and compared with the real heat transfer. Predicted wall temperature and thermal resistance obtained from FEA deviated from 4.25% and 3.63% respectively. He proved that the developed model can provide adequate predictions for heat transfer.

Yong Li et al., 2012 [9] developed a mathematical model for heat pipe with grooved-sintered wick for boiling and condensation which happens in evaporator and condenser respectively. His developed mathematical model is well correlated with the Stranle and Cole [10]. The developed model has a thermal resistance of 0.027 K/W in the condenser section and for the evaporation section, the thermal resistance is ranging from 0.01 to 0.55 K/W. The thermal resistance of the condenser increases more sharply for the first 20-40s because it takes time for liquid circulation to reach the equilibrium condition. the total thermal resistance of the heat pipe is 0.02 to 0.56 K/W.

M.K. Russel et al., [11] studied the effect of different orientation angles of U shaped groove-sintered wick. In this study, he conducted experiments on different inclination and found the best position for the minimum thermal resistance. He explained the grooved wick showed more thermal resistance than the sintered wick. The effect of gravitation was more intense on the grooved than the sintered wick. In an inverted position the capillary effect on the grooved wick was too low that it was not enough for the fluid rise. Maximum Q for grooved and sintered was found to be 47W and 27W respectively

Asghar Alizadehdakhel et al., [12] compared experimentation with the CFD model and got a good agreement. He also mentioned that for further analysis, CFD analysis can be useful. In this study, the fill ratio and heat input effect were determined with experiment and CFD modelling. As the heat input increases the performance of the evaporator decreases and as the fill ratio increases the performance reaches optimum and further increasing thereafter it decreases.

Yuan Zhao al., [13] determined the thermal performance of sintered micro groove wick. The copper powder having a diameter of 50μm and a pore radius of 12μm is used. His experiments showed that grooved wick plays a major role than sintered wick in finding critical heat flux. The results reveal that bi-dispersed could improve the performance of a heat pipe with a mono wick.

Shwin-Chung Wong et al., [14] studied the composite grove mesh in which 200 mesh, deionized water is used. In this study, he proved that the performance of composite mesh is much better compared to the wick he has taken for study. the wick reaches dry out condition when heat input is 45W and only able to perform better when the tilt angle is 30 degrees.

Somasundarumet al., [15] performed experiments on metal foam wick. They assessed the impact of warmth input, rate of cooling water and temperature of condenser side, and the fill ratio of working liquid on the warm productivity of copper level warmth pipe with a wick with 0.77 porosity and 1.114e-10mm2and water as the working liquid. They found that expansion of one and two wick sections to the arrangement leads to a 2.1% and 3.1% decrease in heat obstruction separately.

Hui Li et al., 2018 [16] developed a novel multi-scale composite wick that was proposed for two-phase heat transfer. Capillary studies were studied based on infrared imaging technology and the effects of powder size and nano substrate are studied in deep. His results showed that the larger the powder diameter and irregular shape is good for the rise of liquid. Capillary performance is good for both the fluids but acetone performs better.

Wei Zhong [17] developed the Ergun's equation for flow through the sintered metal porous flow .it is observed that the Ergun equation provides close approximation and can be used for the flow through porous media.

From the literature review, it is evident that heat pipe wick design plays a crucial role in the heat transfer process. It is seen that more work is done on the composite and hybrid wick designs. In this study, the work is done on the

groove-sintered wick design. The aim of this investigation is to trade-off between the capillary pressure and permeability. From the literature, it was found that the sintered wick can generate high capillary rise whereas grooved wick has good permeability. Both the above requirements can be met by composite wick only. Most of the published work is done on experimental studies. A comprehensive CFD simulation is not yet done on fluid flow and heat transfer in the groove-sintered heat pipe.

Regarding the above-mentioned investigations for modeling of the two-phase or phase change using CFD, in the present work it has been tried to model a combination of the two-phase flow with evaporation and condensation in a grove-sintered wick. For this purpose, experiments done by [1] were considered and the CFD modeling is carried out to investigate its performance in different operating conditions.

III.CFD MODELING

The objective of this paper is to design and perform thermal analysis of groove-sintered heat pipe in CFD. Hence, a laminar multiphase stream framework without chemical reaction has been adopted in this thermal analysis. A multiphase flow process contains a mixture of phases assigning phase 1 as water and phase 2 as gas, which are assumed to be mixed at scales much bigger than the molecular scale.

Moreover, the evaporation and condensation of working fluid inside the wick have been carried out by using the volume of fluid (VOF) model. VOF model considers two or more non-miscible fluids by solving a single set of momentum equations (Navier-Stokes) and tracing the volume fraction of each of the fluids throughout the wick. In each cell, the summation of volume fraction is unity. In CFD modeling, Navier-Stokes equations are solved simultaneously. The equations are as follows.
Mass conservation (derived from the continuity equation)

$$\frac{d\rho}{dt} + \rho\left(\vec{\nabla}.\vec{U}\right) = 0 \quad (1)$$

Momentum conservation

$$\rho\frac{D\vec{V}}{Dt} = -\nabla p + \rho\vec{g} + \mu\nabla^2\vec{U} \quad (2)$$

Energy conservation

$$\rho C_v\frac{DT}{Dt} = -P\vec{\nabla}.\vec{U} + \varepsilon\nabla^2 T - \vec{\nabla}.\overrightarrow{Q_r} + Q'' + \Phi \quad (3)$$

Where,

∇= Divergence function
Φ= Heat dissipation function
Q_r= Radiation flux losses
Q''= Internal heat generation rate/unit volume
t = Time function
ρ = Density
$\vec{U}$ = Velocity field function
μ = Dynamic viscosity
ε = Permeability
T = Temperature in K
C_v= Specific heat at constant volume

The flow through the porous media follows Ergan's equation. Following is the Ergun equation for porous medium

$$\frac{|\Delta p|}{L} = \frac{150\mu(1-\epsilon^2)}{D_p^2.\epsilon^3} v_\infty + \frac{1.75\rho(1-\epsilon)}{D_p.\epsilon^3} v_\infty^2 \quad (4)$$

Where,

Δp = Pressure-drop
ϵ = Void fraction
D_p= Mean particle diameter
L = Length of flow field
v_∞ = Free stream velocity

The permeability and inertial resistance are calculated from the below equations

$$\alpha = \frac{D_p^2\epsilon^3}{150(1-\epsilon^2)} \quad (5)$$

$$C = \frac{3.5(1-\epsilon)}{D_p(\epsilon^3)} \quad (6)$$

Where,
α= permeability
C=inertial loss

3.1 GEOMETRY

A 3D geometry has been created in Ansys SpaceClaim 3D CAD design software as shown in figure 1, due to the symmetricity of the heat pipe along the longitudinal axis, the advantage of axis-symmetry has been taken by modeling and simulating half of the plane of the heat pipe wick. The specifications of the heat pipe are mentioned in the table.

Table-1: Specification of heat pipe geometry

Parameter	**Value**
Vacuum	(Pa) 4 *10^4
Working fluid	Purified water
Fill ratio	1
Flattened height H	3.5 mm
Length of the heat pipe	220 mm
Length of the evaporator (La)	35 mm
Length of the condenser (Lc)	65 mm
Number of grooves	55
Thickness of wick	0.3 mm
Powder shape	Spherical powder
Powder diameter	85 µm
Crack height	0.3 mm
Crack width	0.18 mm

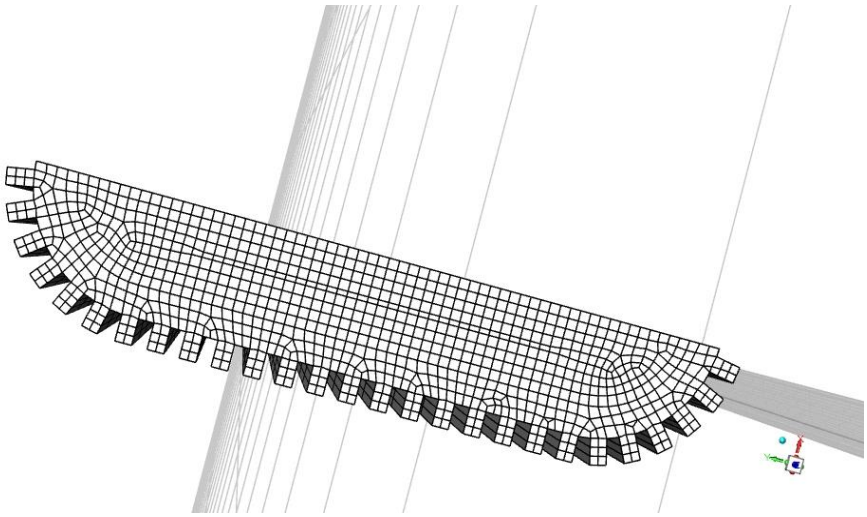

Fig.1 Mesh geometry of heat pipe

4.1. BOUNDARY CONDITIONS

Independency of mesh was done to ensure the results were independent of size. The geometry was created as domain adiabatic fluid, condenser fluid, evaporator fluid, porous adiabatic, porous condenser, and porous evaporator. The total number of nodes and elements are 213525 and 269724 respectively.

Finding the thermal resistance of heat pipe at the different heat flux is the main criteria. The heat flux of 17593, 26408, 45472, 56841, and 68209 W/m^2 (20, 30, 40, 50, and 60 W) is given. The condenser side was given a convective coefficient value making the constant water bath temperature at 45 degrees Celsius. No-slip conditions are given to walls. In fluid dynamics, for viscous fluids, the no-slip condition states that at a solid boundary, the fluid has zero velocity compared to the boundary. The fluid velocity at all solid-fluid boundaries is the same as the solid boundary, hence the velocity for boundary condition will become

$$U_{WALL} = 0 \quad (7)$$

The walls of the condenser and evaporator sections are kept at a constant heat flux. Heat flux is stated across the boundary of the wall. Wall heat flux was the total heat flux through the domain, including convective and radiation. Constant heat flux was given to the adiabatic section of the Groove-sintered wick. We will then need to set the appropriate value for the heat flux at the wall surface in the heat flux field. The adiabatic wall is applied to a total heat flux as zero (i.e., insulated) as the boundary condition. This is the default condition for all walls.

$$Q_w = 0 \quad (8)$$

3.3 SOLUTION

Initially, to validate the results, the porosity is taken as 42%, and the applied heat flux for the heat pipe is 45472W/m2, and the corresponding heat input of 40W. Comparison is made with experimental results and found that the CFD results are aligned with the experimental values. The porosity is then decreased to 35%, as decreasing porosity there is an increase in the capillary rise and can ensure efficient working of the heat pipe. The porosity is increased to 50% and thermal analysis is made with varying heat input. The reason for changing the porosity is by decreasing the porosity creates void and the working fluid can easily seep through the wick. The governing equations are solved using fluent solver ANSYS 20R1. Due to the dynamic behavior of the two-phase flow in a heat pipe, unsteady-state calculations were used with time step and overall time of 0.001 and 450 s respectively. A well-known SIMPLEC algorithm was adopted to solve the pressure–velocity coupling in the Navier-Stokes equations. Backward differencing was implemented for the time and the QUICK scheme was used for the discretization of the governing equations.

IV. RESULTS AND DISCUSSION

CFD simulations are done to obtain the wall temperature profile, velocity profiles, and volume fraction to calculate the thermal resistance of the heat pipe.

4.1. Temperature Distribution:

Wall temperature distributions are determined when porosity and the heat input are varied. The porosity is 42% and the heat input is 40W. Fig 2(a) shows the temperature distribution along the heat pipe. The contour explains the initiation of evaporation of distilled water. The temperature of the evaporator is 310K. The evaporation of fluid is seen more at the walls than at the center of the heat pipe. This is because of high heat transfer near the walls. Fig 2(b) shows the temperature distribution after some time where it is seen that water from the evaporator section is moving towards the condenser section due to the pressure variation. In Fig.2(c) the temperature difference is the same but the temperature in the adiabatic section is seen increasing. Fig. 2(d) shows the adiabatic section where there is no major difference in temperature. The visualization of heat transfer because of phase change is seen and the process continues. In Fig. 2(e) the temperature difference is seen decreasing. Fig. 2(f) and (g) shows the water is returning to the evaporator through the groove-sintered wick and the temperature of the water is about 300K in the condenser. In Fig. 2(h) the heat pipe is seen in a steady state. During the process, the temperature difference between the evaporator and condenser is not exceeding 10K. Thermal resistance is calculated by considering the temperature difference and heat applied.

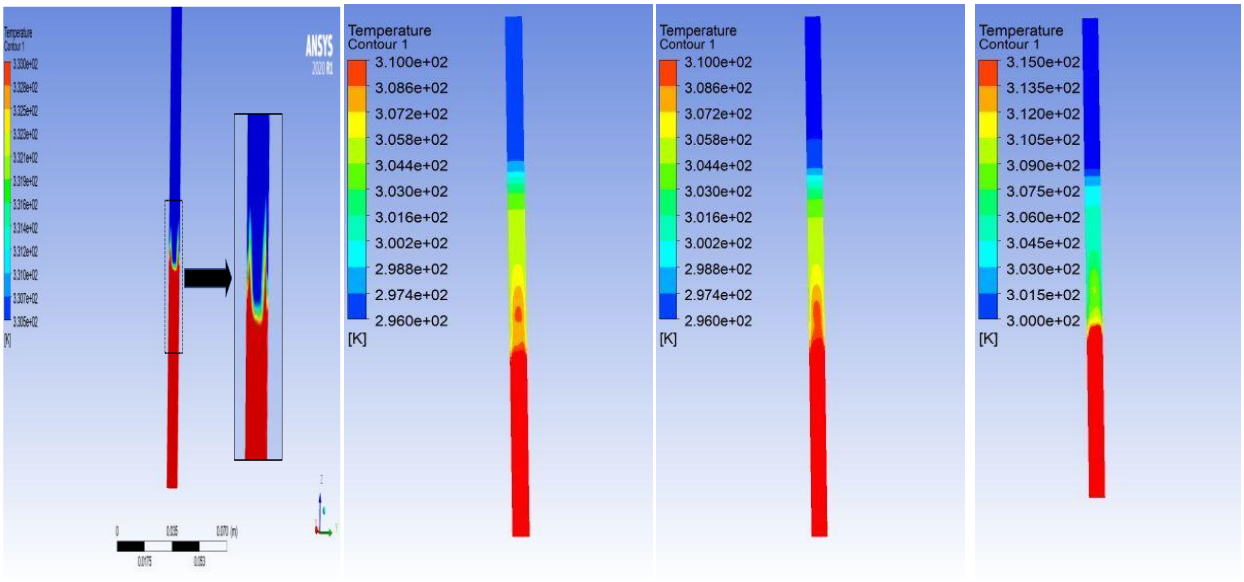

(a) (b) (c) (d)

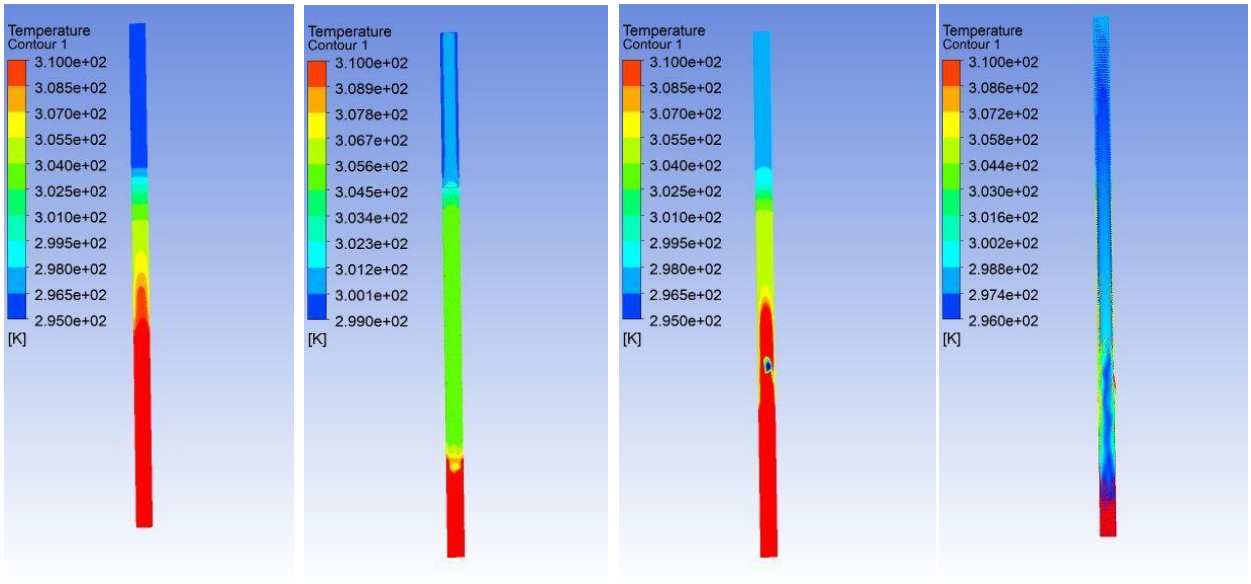

(e) (f) (g) (h)

Fig. 2 Temperature distribution along the heat pipe when porosity is 42% at a heat input of 40W

4.2. Contour of Volume Fraction:

Below part is the evaporator and the top one is the condenser. Fig. 3(a) shows the evaporator is filled with water and the rest of the heat pipe is empty. The fill ratio of the heat pipe is 1 meaning the entire evaporator is filled with water. When the heat is applied in the next time steps, there is a smaller layer of evaporation is seen. In further time steps Fig. 3(b) and (c) explains the evaporation of water. Fig. 3(d) and (e) is the condenser section where it is seen that condensed fluid is coming toward the evaporator section through the wick. Fig. 3(f) and (g) shows the boiling of fluid where water from wick boils and evaporation occurs.

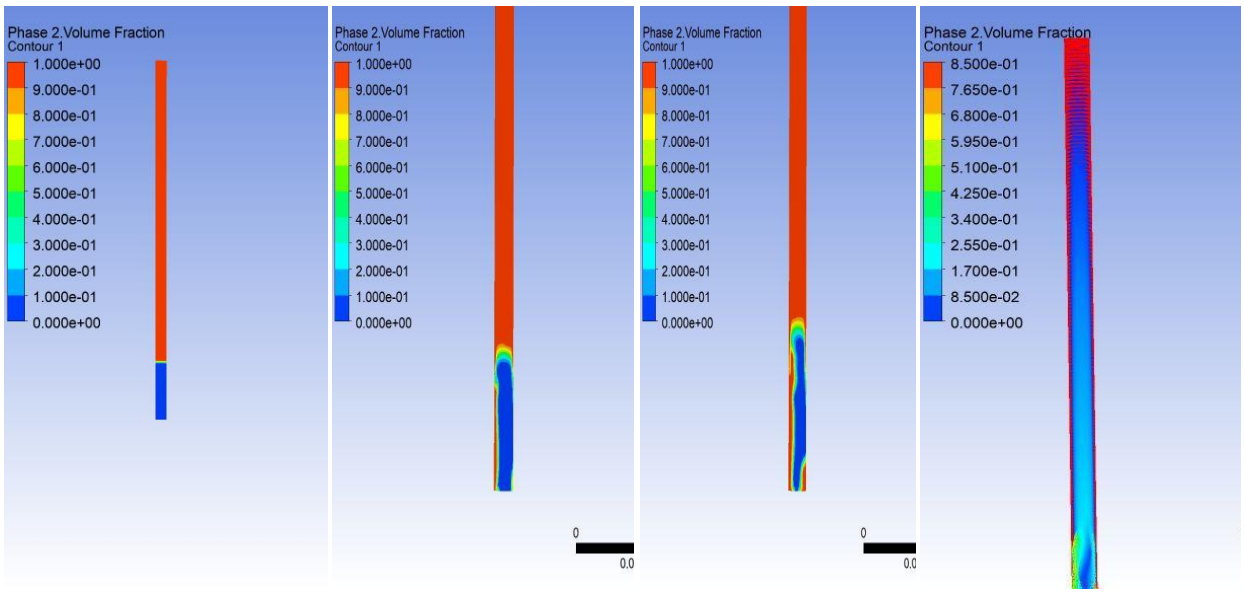

(a) (b) (c) (d)

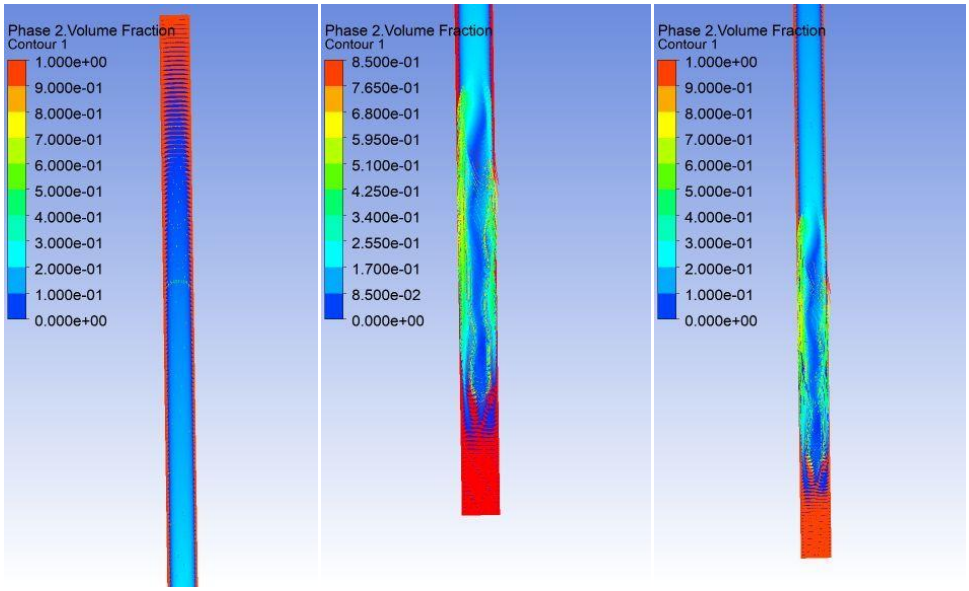

(e) (f) (g)

Fig.3 Contours of volume fraction at different time steps when porosity is 42% at a heat input of 40W

4.3. Contours of Velocity :

The velocity contours are shown below. Fig. 3(a) shows that the velocity of the fluid is high in the evaporator section because of the high evaporation rate. The water vapor is seen moving towards the condenser section faster as there is no restriction and the higher pressure in the evaporator. Fig. 3 (b) shows the velocity vectors. It mainly focuses on the area where the phase change of fluid takes place and it is seen that there is a swirl motion between the water and water vapor exchanging heat. The velocities of water and the water vapor are 0.004 and 0.2 m/s respectively. The velocity of water (phase 1) is low in wick as the flow is taking place in porous wick and water vapor (phase 2) is high. Fig.3 (c) shows the streamlines of flow inside the heat pipe at the evaporator section. The flow seems to be uniform throughout the core region and the velocity is 1.7 m/s. The flow in the wick is varying and the velocity is 1.64 m/s. Fig.3 (d) shows the condensed liquid entering into the wick to reach the evaporator section. The velocity of the fluid is approximately 0.3m/s.

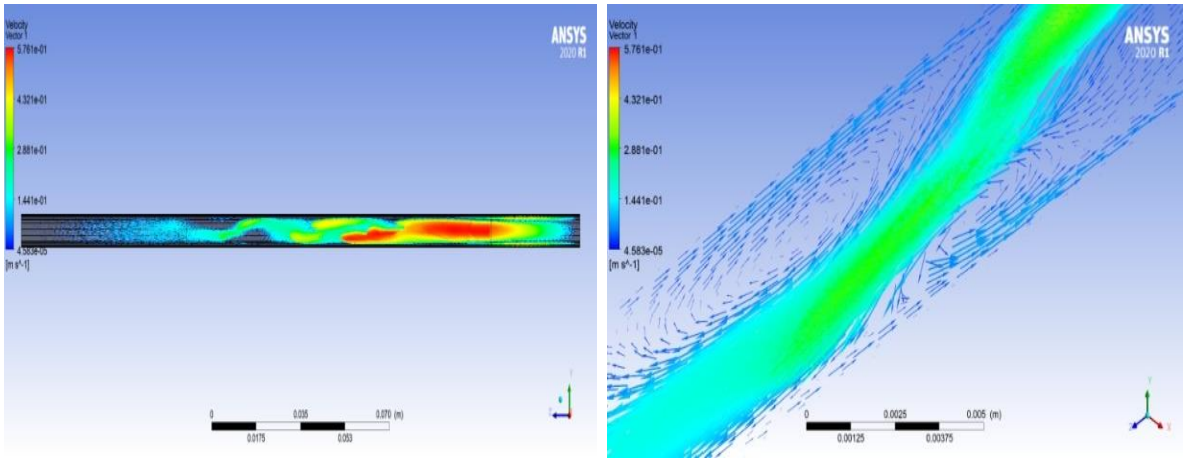

(a) (b)

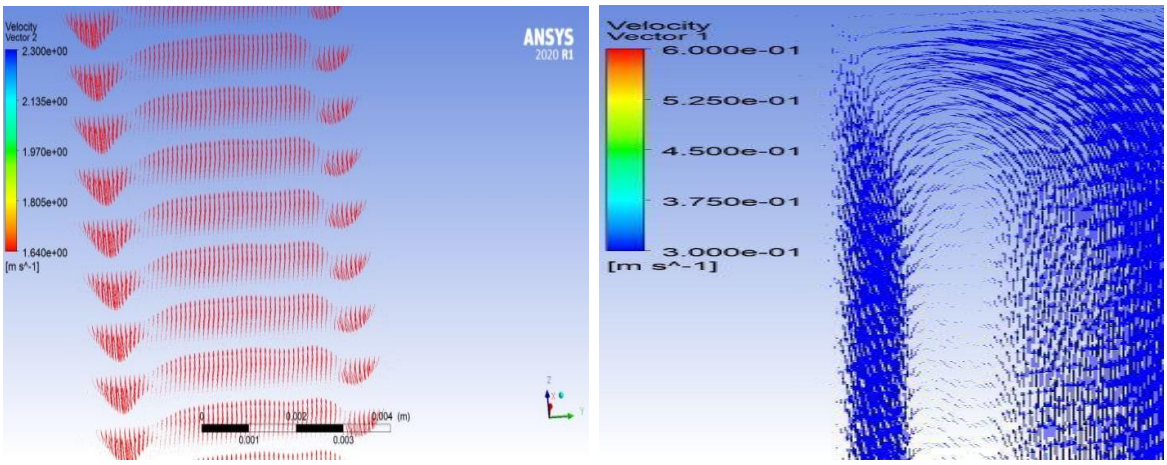

(c) (d)

Fig 3. Contours of velocity

(a) Variation of velocity along the heat pipe; (b) Velocity vectors ;(c) Contours of streamlines; (d) Velocity vectors in the condenser.

4.4. Contours of Streamlines:

The trajectory of fluid in the condenser and evaporator is given below. Fig 4(a) shows the condenser section where the water vapor is exchanging heat with the environment and it gets converted into water. The water is seeping into the evaporator through the wick. In Fig. 4(b) the fluid in the condenser is seen moving in the wick. Fig. 4(c) and (d) shows the streamlines in the evaporation section. At the initial time steps, the evaporator section is filled with water vapor, and as the time steps increase we can see the presence of condensed liquid water in the evaporator.

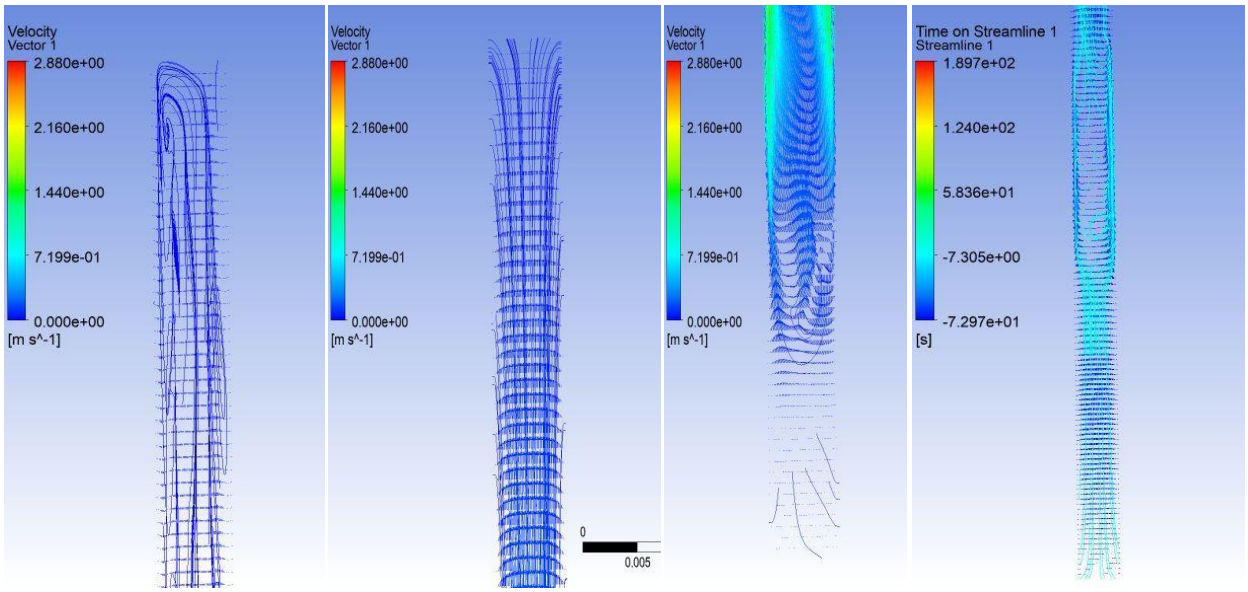

(a) **(b)** **(c)** **(d)**

Fig.4 Contours of streamlines in

(a) Condenser at time 0.05sec (b) Condenser at time 0.2sec (c) Evaporator at time 1sec (d) Evaporator at time 2sec

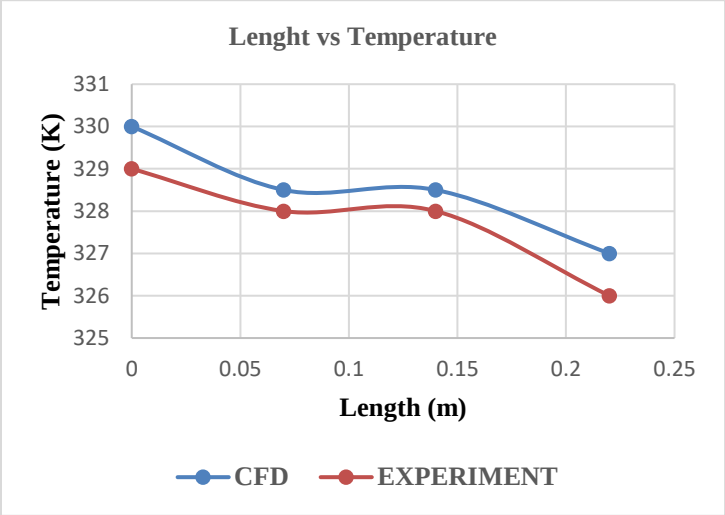

Fig.5 Temperature variation along the heat pipe in CFD analysis and experimentation

A comparison is done between the work done by [1] and the CFD simulation done in this study. A good agreement is seen from the two comparisons of the temperature difference between evaporator and condenser and thermal resistance. According to the experiment, the thermal resistance at the 40W and 50W at porosity 42.1% are 0.049K/W and 0.046 K/W respectively. The temperature difference between the evaporator and condenser is 2 degrees to 2.5 degrees. In this study, firstly the comparison is made between the experimental and CFD analysis in which the error is approximately 2 to 3% error is seen and it is generally because of the temperature variation in the adiabatic section where unpredictability is more.

The lower porosity is better, which will increase the capillary pressure thereby increasing in pressure difference (ΔP) of the heat pipe. A higher-pressure drop is required for efficient working of the heat pipe. The porosity of sintered wick is decreased to 35% keeping the number of grooves constant. Hence void fraction is low. There is also a contradiction that lower porosity decreases the mass flow rate thereby decreasing the heat rejection. By keeping all the parameters in observation the porosity is not further reduced and CFD is performed for the 35% porosity and heat input is varied. Heat input is incrementally increased and results are obtained. The velocity contours and temperature profiles are shown below.

The evaporator was filled with liquid and a heat input of 50W was given at the evaporator end. Fig. 3(a) shows the initial volume fraction and at the initial time step. The time steps are incrementally increased and a change in volume fraction was seen. Small evaporation is seen at the interface between the evaporation and condenser. As the time steps increased there is the formation of vapor and rising towards the condenser section.

The thermal resistance for 40W at 42.1% porosity is 0.0625K/W. Similarly, the remaining calculation for different porosities has been done and graphs are plotted.

The calculated results for thermal resistance are shown in table 2.

Table.2 Thermal resistance for heat input and porosity values

Heat Input (W)	Porosity (35%) (K/W)	Porosity (42.1%) (K/W)	Porosity (50%) (K/W)
20	0.065	0.07	0.079
30	0.045	0.055	0.058
40	0.04	0.045	0.052
50	0.035	0.04	0.045
60	0.031	0.03	0.036
70	0.038	0.044	0.04
80	0.045	0.056	0.05

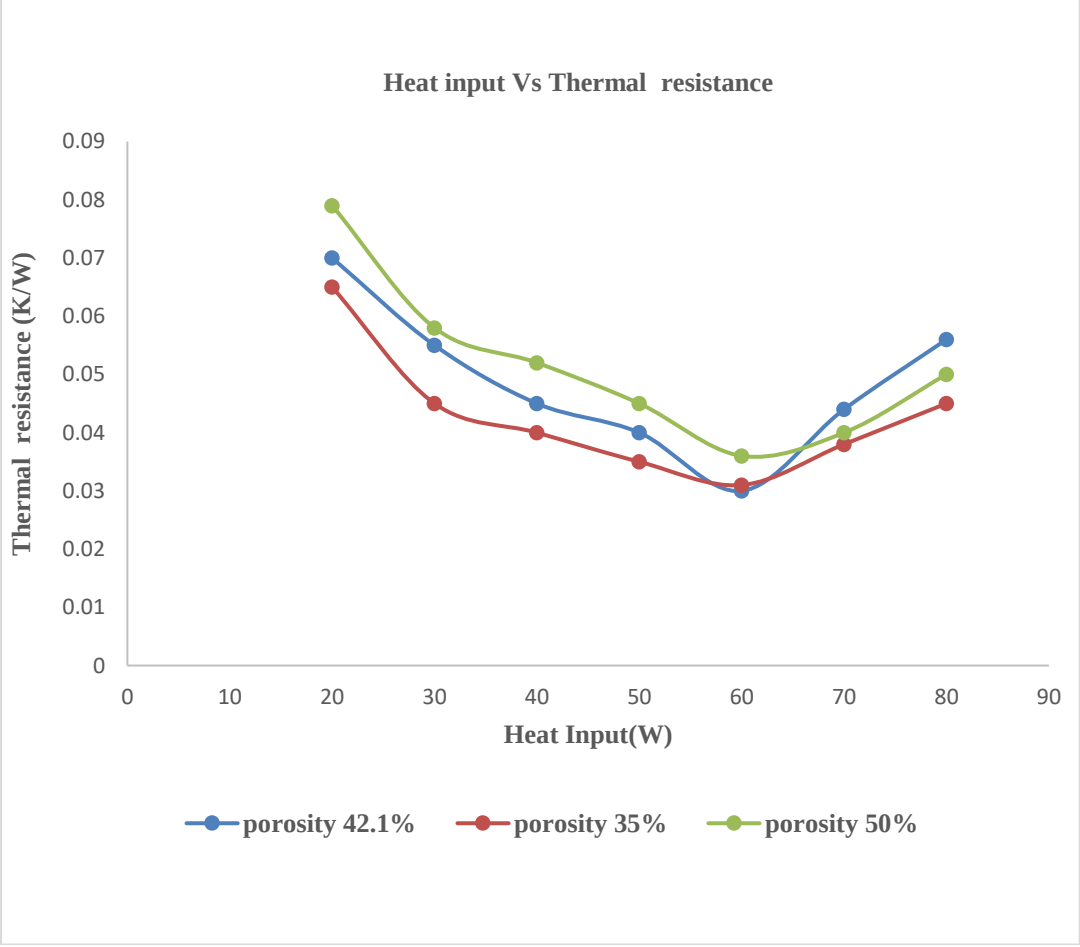

Fig.6 Plot between the thermal resistance and heat input at different porosity values

V.CONCLUSION

In the present work, a comparison is made between the CFD and experimental work. The error between the CFD and experiment is less than 5%. The thermal resistance obtained from the CFD for porosity 35% is low when compared to the porosity 42 and 50%. The velocity, temperature, and volume fraction contour are analyzed and discussed. The maximum heat transfer limit is 60W and after that, it is observed that thermal resistance is increased. Thermal resistance is least for porosity 35% at 60W. From all the cases it can be concluded that optimum porosity always better for minimal thermal resistance. The porosity is not decreased more than 35% because it affects the permeability of working fluid.

REFERENCES

1. Riffat, S. & Ma, Xiaoli. (2007). Recent developments in heat pipe technology and applications: A review. International Journal of Low-carbon Technologies, 162-177/ijlct.
2. Mohamed chaker zaghdoudi, use of heat pipe cooling systems in the electronics industry, www.electronics-cooling.com/2004.
3. L.L.Vasiliev, Micro and miniature heat pipes e electronic component coolers, Applied Thermal Engineering 28 (2008) 266e273.
4. Minghan Zhu, Jin Huang, Mengjie Song, Yanxin Hu, Thermal performance of a thin flat heat pipe with a grooved porous structure, Applied Thermal Engineering, Volume 173,2020,115215, ISSN 1359-4311
5. Lelun Jiang, Yong Huang, Yong Tang, Yan Li, Wei Zhou, Linzhen Jiang, Jinwu Gao, Fabrication and thermal performance of porous crack composite wick flattened heat pipe, Applied Thermal Engineering, Volume 66, Issues 1–2,2014.
6. Jiayin Xu, Dongcheng Wang, Zhuohuan Hu, Li Zhang, Li Ye, Yuren Zhou, Effect of the working fluid transportation in the copper composite wick on the evaporation efficiency of a flat loop heat pipe, Applied Thermal Engineering, Volume 178,2020, 115515, ISSN 1359-4311
7. Yech-Ju Lin and Kuen-Shyang Hwang, Effects of Powder Shape and Processing Parameters on Heat Dissipation of Heat Pipes with Sintered Porous Wicks, Materials Transactions, Vol. 50, No. 10 (2009) pp. 2427 to 2434 The Japan Institute of Metals.
8. T. Naemsai, P. Terdtoon, N. Kammuang-lue, P. Sakulchangsatjatai, Numerical Model of Heat Transfer Characteristics for Sintered-Grooved Wick Heat Pipes under Non-uniform Heat Loads, *AppliedThermal Engineering* (2018).
9. Yong Li, Heng-fei He, Zhi-xin Zeng, Evaporation and condensation heat transfer in a heat pipe with a sintered-grooved composite wick, Applied Thermal Engineering.
10. S.V. Stralen, R. Cole, Boiling Phenomena, McGraw-Hill Inc., New York, 1979.
11. M.K. Russel, C. Young, J.S. Cotton, C.Y. Ching, The effect of orientation on U-shaped grooved and sintered wick heat pipes, Applied Thermal Engineering, Volume 31, Issue 1,2011, Pages 69-76, ISSN1359-4311.
12. Asghar Alizadehdakhel, Masoud Rahimi, Ammar Abdulaziz Alsairafi, CFD modeling of flow and heat transfer in a thermosyphon, International Communications in Heat and Mass Transfer, Volume 37, Issue 3,2010, Pages 312-318, ISSN 0735-1933.
13. Le-lun JIANG, Yong TANG, Wei ZHOU, Lin-zhen JIANG, Long-sheng LU, Fabrication of flatten grooved-sintered wick heat pipe, Trans. Nonferrous Met. Soc. China 23(2013) 2714−2725.
14. Wei-Wei Wang, Yang Cai, Run-Zhe Liu, Fu-Yun Zhao, Di Liu,Experimental and numerical investigations of a radial heat pipe for waste heat recovery,Applied Thermal Engineering,Volume 154,2019,Pages 602-613,ISSN 1359-4311
15. D. Somasundaram, A. Mani, M. Kamaraj, Experimental Investigation of Thermal Performance of Metal Foam Wicked Flat Heat Pipe, Experimental Thermal and Fluid Science (2016).
16. Hui Li, Shengjuan Fu, Gongfa Li, Ting Fu, Rui Zhou, Yong Tang, Biao Tang, Yong Deng, Guofu Zhou,Effect of fabrication parameters on capillary pumping performance of multi-scale composite porous wicks for loop heat pipe,Applied Thermal Engineering,Volume 143,2018,Pages 621-629,ISSN 1359 4311.
17. Wei Zhong, Ke Xu, Xin Li, Yuxuan Liao, Guoliang Tao, Toshiharu Kagawa, Determination of pressure drop for airflow through sintered metal porous media using a modified Ergun equation, Advanced Powder Technology, Volume 27, Issue 4,2016, Pages 1134-1140, ISSN 0921-8831